the reaction mixture, giving a lavender solution. Chilling to −20 °C precipitated shiny green crystals of **48** (0.28 g, 50%): ^{1}H NMR ($CDCl_3$) δ 8.66 (m, 4 H), 7.20 (m, 4 H), 7.20 (m, 4 H); IR (KBr) 1605, 1555, 1500 cm^{-1}; $\lambda_{max}^{CH_2Cl_2}$ (log ε) 345 (4.24), 587 nm (4.56); FDMS, m^+/e 552 ($C_{17}H_8Cl_4F_2O_2{}^{130}Te$), 482 ($M^+$ − 2 Cl). Anal. Calcd for $C_{17}H_8Cl_4F_2O_2Te$: C, 37.0; H, 1.5. Found: C, 37.3; H, 1.6.

Registry No. **2a**, 108743-34-6; **9**, 34108-71-9; **16**, 87761-66-8; **17**, 87761-67-9; **18**, 108743-24-4; **19**, 91412-35-0; **20**, 108743-25-5; **22a**, 108743-33-5; **22a** ethyl ester, 108743-35-7; **23a**, 101009-47-6; **23b**, 91412-62-3; **23c**, 108743-36-8; **24**, 91412-33-8; **25**, 108743-26-6; **26**, 91412-34-9; **27**, 91412-35-0; **28**, 108743-27-7; **29**, 91412-37-2; **30**, 91412-38-3; **31**, 108743-28-8; **32**, 108743-29-9; **33**, 91412-39-4; **34**, 108743-30-2; **35**, 108743-31-3; **36**, 91412-40-7; **37**, 108743-32-4; **38**, 91412-45-2; **39**, 91412-46-3; **40a**, 84144-41-2; **40b**, 84144-47-8; **41**, 91412-42-9; **43**, 91412-43-0; **44**, 87761-70-4; **45**, 87761-71-5; **46**, 87761-72-6; **47**, 87761-73-7; **48**, 91412-54-3; **49**, 108772-63-0; **50**, 91412-53-2; **51**, 108743-37-9; **52**, 108743-38-0; **53**, 108743-39-1; **54**, 108743-40-4; **55**, 108743-41-5; **56**, 108743-42-6; **57**, 21737-87-1; **58**, 91412-48-5; PhC(O)Cl, 98-88-4; AcCl, 75-36-5; *p*-$NO_2C_6H_4CO)Cl$, 122-04-3; *p*-$CNC_6H_4C(O)Cl$, 6068-72-0; *p*-$FC_6H_4C(O)Cl$, 403-43-0; Ethyl tetrolate, 4341-76-8; *p*-anisoyl chloride, 100-07-2; 2,4-dinitrobenzoyl chloride, 20195-22-6; 3,5-dinitrobenzoyl chloride, 99-33-2; 2-furanacryloyl chloride, 20689-54-7; 2-thiopheneacryloyl chloride, 28424-61-5.

Mechanism of the Light-Assisted Nucleophilic Acylation of Activated Olefins Catalyzed by Vitamin B_{12}

Lorenz Walder* and Richard Orlinski

Institute of Organic Chemistry, University of Berne, Freiestrasse 3, CH-3012 Berne, Switzerland

Received April 3, 1986

The conjugate addition of acyl groups to C–C double bonds, by a vitamin B_{12} catalyzed electrochemical reduction of acetic anhydride in the presence of Michael olefins and under visible light, is shown to involve sequential formation and cleavage of the Co–C bond in acetylcobalamin. Photolysis of this intermediate takes place efficiently only in the presence of the activated olefin. The rate constant of acylation of B_{12s} by acetic anhydride (k_1 = 0.017 M^{-1} s^{-1}), the quantum yield of the visible light induced cleavage of the Co–C bond ($\Phi \approx 0.35$), and the relative rate of acylation of a series of activated olefins were determined electrochemically from catalytic currents. These values are comparable with independently measured k values for the isolated reaction steps. The k values for the acetyl-transfer reaction correlate well with the reduction potentials of the activated olefins or with their σ_p^-, exhibiting a linear free energy relationship (ρ = 2.3). The transferred acyl moiety reacts as a Co-stabilized nucleophilic radical and not as a "free" radical.

There exists a broad interest in simple and mild methods for the synthesis of 1,4-dioxo compounds. Their retrosynthetic disconnection, as shown in eq 1, leads to a Michael acceptor and an acyl anion. The associated chemical problem consists in stabilizing the negative charge on the C atom of the carbonyl function to the extent that side reactions are avoided but nucleophilic reactivity persists. Reagents with masked functionality[1] and acylmetallic compounds have been found to meet these conditions. In the latter case, limited synthetic use has been reported for group Ia, IIa, and IIIb derived acyl anions due to their uncontrollably high reactivity.[2a] Improved stability has recently been noted for acyl anions produced from acyl chlorides and SmI_2.[2b] Nucleophilic acylation of activated olefins by formal acyl anions bound to transition metals are reported for acylcuprates,[2c] acyltetracarbonyliron,[2d] and acylnickelates.[2e] Their preparation, by sequential insertion of CO and activated olefin into metal–carbon bonds, is not suited for catalytic applications. On the other hand, so-called "free" radicals are known to exhibit sufficient nucleophilic reactivity for Michael-type reactions.[3] Recently Scheffold and co-workers have shown that under mild reductive conditions vitamin B_{12} (**1**) is an excellent catalyst for the 1,4 addition of carboxylic anhydrides to activated olefins[4a] (eq 2). An intermediate acylcobalamin (**2**) is

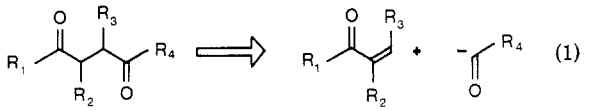

(1)

Scheme I. Catalytic Cycle. B_{12}-Catalyzed Acetylation of Activated Olefins under Visible Light Illumination and Reducing Conditions

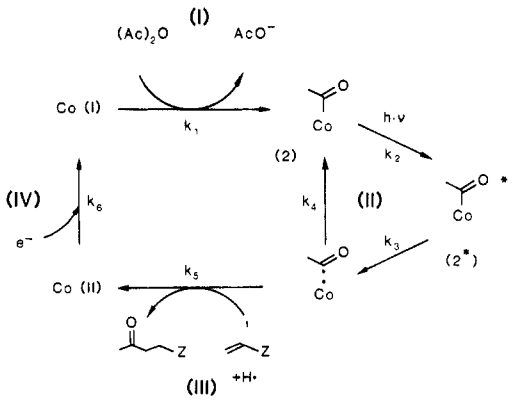

$$R^2R^3C{=}CR^1Z + (R^4CO)_2O + H^\bullet + e^- \xrightarrow[-1.0\ V,\ h\nu,\ or\ -1.6\ V]{vitamin\ B_{12}} (R^4CO)R^2R^3C{-}CHR^1Z + R^4CO_2^- \quad (2)$$

Z = electron-withdrawing group

(1) (a) Stetter, H. *Angew. Chem.* **1976**, *88*, 695. (b) Hase, T. A.; Koskimies, J. K. *Aldrichim. Acta* **1981**, *14*, 73.

(2) (a) Lever, O. W. *Tetrahedron* **1976**, *32*, 1943. (b) Souppe, J.; Namy, J.-L.; Kagan, H. B. *Tetrahedron Lett.* **1984**, *25*, 2869. (c) Seyferth, D.; Hui, R. C. *J. Am. Chem. Soc.* **1985**, *107*, 4551; *Tetrahedron Lett.* **1986**, *27*, 1473. (d) Cooke, M. P.; Parlman, R. M. *J. Am. Chem. Soc.* **1977**, *99*, 5222. (e) Corey, E. J.; Hegedus, L. S. *J. Am. Chem. Soc.* **1969**, *91*, 4926.

(3) (a) Bellatti, M.; Caronna, T.; Citterio, A.; Minisci, F. *J. Chem. Soc., Perkin Trans. 2* **1976**, 1835. (b) Gottschalk, P.; Neckers, D. C. *J. Org. Chem.* **1985**, *50*, 3498.

0276-7333/87/2306-1606$01.50/0

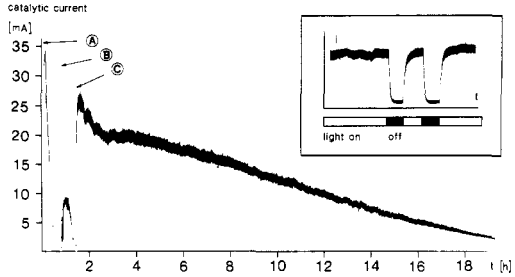

Figure 1. Catalytic current ($i_{cat.}$)–time curve for the B_{12}-catalyzed acetylation of **3c** in DMF/0.1 M $LiClO_4$ at −1.0 V (vs. SCE) under white light illumination: A, 0.2 mmol of **1**; B, 6.8 mmol of $(Ac)_2O$; C, 7.6 mmol of **3c**. Coulometry depends slightly on substrates and amine content of solvent: $n_e \approx 1.2$–1.4 on the basis of $(Ac)_2O$ consumed. Inset: light chopped response of $i_{cat.}$.

formed in the reaction by oxidative addition of the anhydride to vitamin B_{12s} (Co(I)). This organometallic species contains a highly stabilized acyl anion. In contrast to the acylmetallic compounds described before, it becomes nucleophilic only upon photoexcitation or reduction[5] and is then transferred to an activated olefin (AO). Co(I) is reformed at the electrode. The current observed has definitely a catalytic character; i.e., it either decreases linearly with time when limited by one of the substrates or it remains constant when limited by the flux of absorbable photons (Figure 1). A plausible mechanism for the light-assisted catalytic cycle is given in Scheme I.

We present here kinetic data for the reaction steps in Scheme I. These were obtained from current measurements by using the same experimental conditions as those developed for the synthetic applications.[4] The rate constants determined by this technique were checked against well-established methods on the same isolated steps. The mechanistic model that best fits our data consists of two generally accepted steps (I and IV) and two complicated and still not well-understood reaction sequences (II and III). Particularly, the existence of an intermediate Co(II)-stabilized alkyl (or acyl) radical is controversial. Such an intermediate has been postulated on the basis of ESR measurements.[6a–d] The quantum yield for the (irreversible) photolysis of alkylcobalamins seems to be strongly influenced by electrophilic substrates,[8] indicating competition between the re-formation of the Co–C bond and an electrophilic attack by the scavenger. Flash photolysis experiments indicate that intermolecular stabilization of the radicals may be effective, i.e., scavenging of free radicals by Co(II),[7b] but lifetimes for intermediate Co-stabilized radicals are not sufficiently long for bimolecular reactions to occur at rates below diffusion control.[7a]

In our study acetylcobalamin underwent photolysis only in presence of both light and electrophilic substrates ($i_{cat.}$ goes from background values to 25 mA upon substrate addition (Figure 1) and absorbance by **2** persists under illumination unless substrate is present (Figure 7)). The rate of photolysis seems to be independent of free Co(II) concentration (no deviation of the zero-order decomposition is observed under continuous illumination in presence of a Michael acceptor). As a working hypothesis we assumed, therefore, a Co(II)-stabilized acyl radical that persists long enough to undergo a bimolecular reaction with an activated olefin (reaction 5, Scheme I). We then checked an alternative mechanism that does not require a long-lived intermediate, i.e., ground-state complexation of acetylcobalamin by the olefin.

The main purpose of this study is to determine quantitatively the reactivity of the acyl moiety in acetylcobalamin after photoexcitation. However, the method developed here allows us to calculate the rate constant for any rate-limiting step in the catalytic cycle.

Kinetic Model of Catalysis

The steady-state approach applied to Scheme I leads to a general expression describing the overall rate in terms of a catalytic current ($i_{cat.}$) as a function of single-step kinetics, i.e., substrate and catalyst concentrations, rate constants, light intensity, quantum yield, and electrochemical parameters (eq 17). Step I: the acetylation of vitamin B_{12s} (Co(I)) by $(Ac)_2O$[5a] is formulated as an irreversible reaction, first order in both [Co(I)] and [$(Ac)_2O$], proceeding throughout the solution. Step II consists of light absorption by **2**[9] (reaction 2) leading (partially) to a photoexcited state (**2***) from which efficient first-order homolysis occurs to yield the intermediate Co···Ac (reaction 3). This species either follows the shunt (reaction 4) and recombines to **2** (treated as an intramolecular, first-order reaction) or reacts with an activated olefin (AO) (reaction 5). The amount of light absorbed per unit time by **2** (I') generally is only a fraction of the intensity entering the solution (I) due to competitive absorption by all other B_{12} intermediates (eq 3). With the assumption that $\epsilon_2 = \epsilon_{Co(II)} = \epsilon_{Co(I)}$, the filter effect is approximated by eq 4 and the rate law for the photoexcitation step is expressed by eq 5 with v_c = cell volume and $\Phi = n\,\mathbf{2}^*$ formed per n photons absorbed by **2**. Step III: the transfer of the acetyl group

$$I' = I\epsilon_2[\mathbf{2}]/(\epsilon_{Co(I)}[Co(I)] + \epsilon_{Co(II)}[Co(II)] + \epsilon_2[\mathbf{2}]) \quad (3)$$

$$I' = I[\mathbf{2}]/[B_{12}] \quad (4)$$

$$d[\mathbf{2}^*]/dt = k_2[\mathbf{2}] = I'\Phi/v_c = I\Phi[\mathbf{2}]/v_c[B_{12}] \quad (5)$$

$$k_2 = I\Phi/nB_{12} \quad (6)$$

and a formal H· to an activated C–C double bond is assumed to proceed irreversibly with a rate governed exclusively by the interaction of Co···Ac and activated olefin. Step IV: electrochemical regeneration of Co(I) takes place irreversibly and is diffusion-controlled at a 300-mV overpotential (eq 7 and 8) with i_l = diffusion-limited current,

(4) (a) Scheffold, R.; Orlinski, R. *J. Am. Chem. Soc.* **1983**, *105*, 7200. (b) For a recent review on B_{12} and related Co complexes as catalysts in organic synthesis, cf.: Scheffold, R.; Rytz, G.; Walder, L. In *Modern Synthetic Methods*; Scheffold, R., Ed.; Wiley-Interscience: New York, 1983; Vol. 3. (c) Scheffold, R. *Chimia* **1985**, *39*, 203.

(5) Actually, acylcobalamins or acylated B_{12} model compounds neither irradiated nor reduced exhibit electrophilic reactivity[5b–d] and have been used for synthesis of unsymmetrical ketones.[5c] (a) Müller, O.; Müller, G. *Biochem. Z.* **1962**, *336*, 299. (b) Bernhauer, K.; Irion, E. *Biochem. Z.* **1964**, *339*, 530. (c) Tabushi, I.; Seto, K.; Kobuke, Y. *Tetrahedron* **1981**, *37*, 863. (d) Yamada, R.-H.; Umetani, T.; Shimizu, S.; Fukui, S. J. *Vitaminology* **1968**, *14*, 316.

(6) Separation between Co· and ·R has been calculated from the band structure of ESR spectra.[6c,d] (a) Ghanekar, V. D.; Lin, R. J.; Coffman, R. E.; Blakley, R. L. *Biochem. Biophys. Res. Commun.* **1981**, *101*, 215. (b) Schepler, K. L.; Dunham, W. R.; Sands, R. H.; Fee, J. A.; Abeles, R. H. *Biochim. Biophys. Acta* **1975**, *397*, 510. (c) Rao, D. N. R.; Symons, C. R. *J. Chem. Soc., Perkin Trans. 2* **1983**, 187. (d) Pezeshk, A.; Coffman, R. E. *J. Chem. Soc., Dalton Trans.* **1985**, 891.

(7) (a) Endicott, J. F.; Netzel, T. L. *J. Am. Chem. Soc.* **1979**, *101*, 4000. (b) Endicott, J. F.; Ferraudi, G. J. *J. Am. Chem. Soc.* **1977**, *99*, 243. (c) Lerner, D. A.; Bouneau, R.; Giannotti, C. *J. Photochem.* **1979**, *11*, 73.

(8) In earlier reports an increased rate of methylcobalamin photolysis was noted in presence of oxygen,[8a] homocystein,[8b] and *p*-benzoquinone.[8c] (a) Pratt, J. M. *J. Chem. Soc.* **1964**, 5154. (b) Yamada, R.; Kato, T.; Shimizu, S. *Biochem. Biophys. Acta* **1966**, *117*, 13. (c) Yamada, R.; Shimizu, S.; Fukui, S. *Ibid.* **1966**, *124*, 195. More recently typical radical scavenger have been used as photolysis-enhancing substrates.[8d,e] (d) Maillard, P.; Giannotti, C. *Can. J. Chem.* **1982**, *60*, 1402. (e) Joblin, K. N.; Johnson, A. W.; Lappert, M. F. *J. Chem. Soc., Chem. Commun.* **1975**, 441.

(9) For studies on the excited state of metallocorrins, see: (a) Vogler, A.; Hirschmann, R.; Otto, H.; Kunkely, H. *Ber. Bunsenges. Phys. Chem.* **1976**, *80*, 420. (b) Gardiner, M.; Thomson, A. J. *J. Chem. Soc., Dalton Trans.* **1974**, 820.

$$dQ/dt = i_l = n_e FAD[\mathrm{Co(II)}]/\delta \quad (7)$$

$$d[2]/dt = k_6[\mathrm{Co(II)}] = i_l/v_c n_e F \quad (8)$$

A = electrode surface, D = diffusion coefficient, and δ = diffusion layer thickness. Steady-state conditions lead to eq 9–14, which are then solved for [CoI] to give eq 15.

$$d[\mathrm{Co(I)}]/dt = 0 = k_6[\mathrm{Co(II)}] - k_1[\mathrm{Co(I)}][(\mathrm{Ac})_2\mathrm{O}] \quad (9)$$

$$d[2]/dt = 0 = k_1[\mathrm{Co(I)}][(\mathrm{Ac})_2\mathrm{O}] + k_4[\mathrm{Co{\cdots}Ac}] - k_2[2] \quad (10)$$

$$d[2^*]/dt = 0 = k_2[2] - k_3[2^*] \quad (11)$$

$$d[\mathrm{Co{\cdots}Ac}]/dt = 0 = k_3[2^*] - (k_5[\mathrm{AO}] + k_4)[\mathrm{Co{\cdots}Ac}] \quad (12)$$

$$d[\mathrm{Co(II)}]/dt = 0 = k_5[\mathrm{Co{\cdots}Ac}][\mathrm{AO}] - k_6[\mathrm{Co(II)}] \quad (13)$$

$$[\mathrm{B}_{12}] = [\mathrm{Co(I)}] + [2] + [2^*] + [\mathrm{Co{\cdots}Ac}] + [\mathrm{Co(II)}] \quad (14)$$

$$1/k_1[\mathrm{Co(I)}][(\mathrm{Ac})_2\mathrm{O}] = (1/k_1[(\mathrm{Ac})_2\mathrm{O}] + k_4/k_2k_5[\mathrm{AO}] + 1/k_3 + k_4/k_3k_5[\mathrm{AO}] + 1/k_5[\mathrm{AO}] + 1/k_6)/[\mathrm{B}_{12}] \quad (15)$$

When i_l is replaced by $i_{cat.}$, the reciprocal forward rates in step I and IV (eq 7 and 8) can be formulated according eq 16. Equations 15 and 16 finally lead to eq 17 describing the overall rate of catalysis.

$$1/k_1[\mathrm{Co(I)}][(\mathrm{Ac})_2\mathrm{O}] = v_c n_e F/i_{cat.} \quad (16)$$

$$\frac{1}{i_{cat.}} = \frac{1}{n_e F n \mathrm{B}_{12}}\left(\frac{1}{k_1[(\mathrm{Ac})_2\mathrm{O}]} + \frac{n\mathrm{B}_{12}}{I\Phi} + \frac{k_4 n\mathrm{B}_{12}/I\Phi + k_4/k_3 + 1}{k_5[\mathrm{AO}]} + \frac{1}{k_3} + \frac{v_c\delta}{AD}\right) \quad (17)$$

Results and Discussion

Equation 17 predicts a linear relationship between $1/i_{cat.}$ and either of the variables $1/I$, $1/[(\mathrm{Ac})_2\mathrm{O}]$, or $1/[\mathrm{AO}]$. Furthermore, it correlates the slopes of corresponding plots to rate constants and quantum yields of individual steps in the proposed catalytic cycle (Scheme I). The successful application of eq 17 depends crucially on achieving steady-state conditions before current measurements are performed. The electrochemical step sets a lower time limit of at least 10 min ($k_6 = 3.6 \times 10^{-3}$ s^{-1}) for the leveling of $i_{cat.}$ into a new steady state after any change in I, $[(\mathrm{Ac})_2\mathrm{O}]$, or [AO]. A valuable test for the absence of side reactions or shunts that are not included in Scheme I is whether $i_{cat.} \to 0$ as $I \to 0$, as $[(\mathrm{Ac})_2\mathrm{O}] \to 0$, or as $[\mathrm{AO}] \to 0$.

Light Intensity and Wavelength Dependence of $i_{cat.}$. Determination of Φ from Catalytic Currents. The influence of light in the B_{12}-catalyzed acetylation of acrylonitrile becomes apparent from the light-chopped current response in Figure 1. From eq 17 the dependence of the reciprocal catalytic current on intensity and wavelength is described by eq 18, where C_1 represents a constant term. If $k_5[\mathrm{AO}] \gg k_4$, eq 18 simplifies to eq 19 and a plot of $1/i_{cat.}$ vs. $1/I_\lambda$ should be linear with slope $1/n_e F\Phi_\lambda$.

$$1/i_{cat.} = (1/I_\lambda \Phi_\lambda n_e F)(1 + k_4/k_5[\mathrm{AO}]) + C_1 \quad (18)$$

$$1/i_{cat.} = 1/I_\lambda n_e F \Phi_\lambda + C_1 \quad (19)$$

Figure 2 shows that an experimental nonlinear $i_{cat.}$ vs. I_{rel} plot becomes linear if the same set of data is represented according to $1/i_{cat.}$ vs. $1/I_{rel}$. Linearity has been observed over more than a decade of the current scale by using white light of known relative intensity or monochromatic light of known absolute intensity. The slope of the latter was used to calculate $\Phi_{490} = 0.35$ (with $n_e = 1.2$). The wavelength dependence of Φ was studied stepwise from 640 to 370 nm (Figure 3). No detectable change of Φ is noted in this range: at long wavelengths $i_{cat.}$ follows the absorption curve of **2** due to incomplete absorption of low-energy light. Between 520 and 320 nm the expected, approximately linear, decrease of $i_{cat.}$ is observed for a constant energy photon flux.

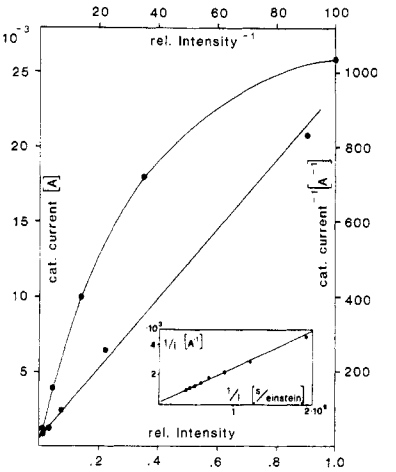

Figure 2. Plot of $i_{cat.}$ vs. relative white light intensity (I) and $1/i_{cat.}$ vs. $1/I$. Inset: monochromatic illumination (490 nm, (0.19–2.67) × 10^{-8} einstein/s).

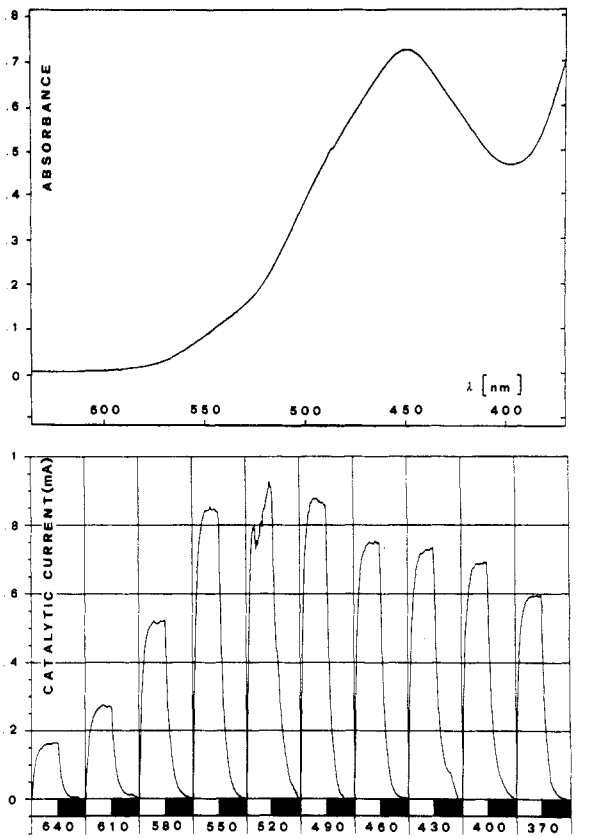

Figure 3. Visible spectrum of **2** and wavelength dependence of $i_{cat.}$ (corrected for background current). Cell alternatively in the dark and illuminated with monochromatic light of stepwise decreasing wavelength and constant energy (1.54 × 10^{-8} einstein/s at 405 nm).

Rate of Acetylation of Vitamin B_{12s} Determined from $i_{cat.}$. If $[(\mathrm{Ac})_2\mathrm{O}]$ is the only independent variable, eq 17 simplifies to eq 20. Experimentally $1/i_{cat.}$ vs. $1/[(\mathrm{Ac})_2\mathrm{O}]$ plots gave straight lines (slope = 2.55 M A^{-1}, r = 0.9998), and hence, from eq 20, $k_1 = 0.017$ M^{-1} s^{-1}. This

$$1/i_{cat.} = (1/n_e F n \mathrm{B}_{12})(1/k_1)(1/[(\mathrm{Ac})_2\mathrm{O}]) + C_2 \quad (20)$$

Table I. Kinetic Data for Acetyl Transfer from Acetylcobalamin to $ZR_1C{=}CR_2R_3$ and Reduction Potentials of the Activated Olefins (AO)

entry	R_1	R_2	R_3	Z	$E_{1/2}$(AO)	log rel k_5	Φ_{max}	log k_5/k_4[a]
3a	H	H	H	COH	−1.65	+0.55		
3b				$COCH_3$	−1.91	+0.046		
3c				CN	−2.05	−0.025	0.47 ± 0.1	~2.5
3d[b]	CH_3				−2.29	−0.66	0.35 ± 0.1	~1.9
3e	H			$COOCH_2CH_3$	−2.06	−0.37	0.45 ± 0.1	~2.0
3f	CH_3				−2.12	−0.32		
3g	H			$CONH_2$	−2.55	−0.59		
4a		CH_3		COH	−1.92	−0.66	0.45 ± 0.1	~1.6
4b	CH_3				−2.04	−0.93		
4c	H	H	$-(CH_2)_2CO-$		−2.11	−1.07		
4d			$-(CH_2)_3-$		−2.07	−1.13		
4e		CH_3	H	$COOCH_2CH_3$	−2.34	−1.26	0.39 ± 0.1	~1.1
5a			CH_3	COH	−2.01	−1.85		
5b				$COCH_3$	−2.18	−2.34		
5c				$COOCH_2CH_3$	−2.47	−2.6		
5d				CN	−2.59	−2.33		

[a] $\log k_5/k_4 = -\log [AO]_{\Phi_{max}/2}$ (eq 24). [b] Mixture of $R_1 = CH_3$, $R_2 = R_3 = H$ and $R_2 = CH_3$, $R_1 = R_3 = H$.

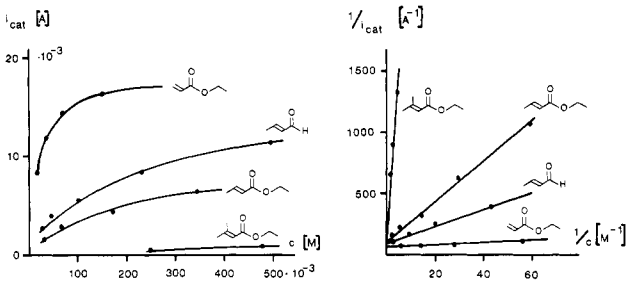

Figure 4. Plot of $i_{cat.}$ vs. activated olefin concentrations [AO] (left) and $1/i_{cat.}$ vs. 1/[AO] (right). From the slopes of the best-fit straight lines relative k_5 was calculated.

value compares well with $k_1 = 0.021$ M^{-1} s^{-1} determined by cyclic voltammetry from the disappearance of Co(I) upon addition of $(Ac)_2O$ to a solution of vitamin B_{12s} (see Experimental Section).

Relative Rates of Acetylation of Activated Olefins Determined from $i_{cat.}$. When [AO] is defined as an independent variable in eq 21, it follows that only relative k_5 values (rel k_5) can be found from the slopes of the $1/i_{cat.}$ vs. 1/[AO] plots (C_3 and C_4 are constant terms). Ex-

$$1/i_{cat.} = C_3 + C_4/k_5[AO] \quad (21)$$

$$\text{rel } k_5 = k_5/C_4 \quad (22)$$

perimental linearity for the reciprocal representation is observed for the current range between 1 and 17 mA corresponding to a concentration range from 2×10^{-2} to 1 M ($r \geq 0.990$). Relative k_5 values (eq 22) for different Michael acceptors (**3a–g**, **4a–e**, **5a–d**) are reported in Table I. These values are very sensitive to the degree of substitution at the β-position (R_2, R_3) and to changes in the electron-withdrawing group. In order to distinguish between the influence of electronic and steric effects in the activated olefins on the rate constant, we measured their polarographic reduction potential under experimental conditions similar to those of the catalytic experiment ($E_{1/2}$ in Table I).[10] In a logarithmic plot of the relative k_5 values vs. $-E_{1/2}$, three classes of activated olefins, β-unsubstituted (**3**), β-monosubstituted (**4**), and β,β-disubstituted (**5**), exhibit linear free energy relationships (Figure 5). The slopes of **3** (−1.35, $r = 0.91$) and **4** (−1.32, $r = 0.89$) are almost identical and correlate well with straight lines,

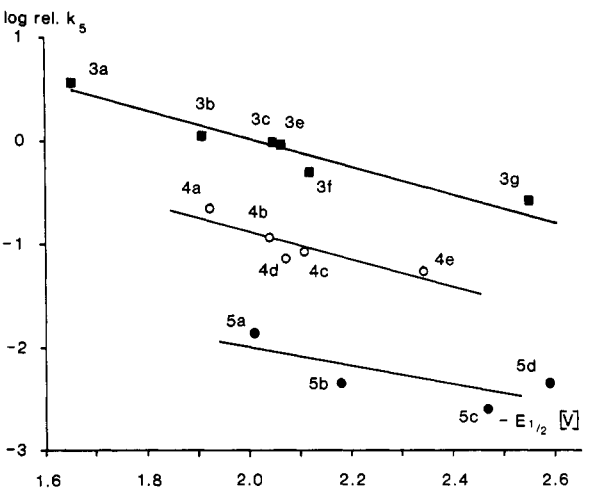

Figure 5. Correlation of log rel k_5 vs. $-E_{1/2}$ of corresponding activated olefin. Classes **3**, **4**, and **5** exhibit LFER with slopes of −1.35 ($r = 0.91$), −1.32 ($r = 0.89$), and −0.88 ($r = 0.75$), respectively.

whereas the few points of **5** scatter (slope = −0.88, $r = 0.75$). The negative sign of the slopes indicates negative charge accumulation on the activated olefin in the transition state. Hence the transferred acetyl moiety has nucleophilic character. Rate constants for nucleophilic, so-called "free (alkyl) radical" additions to activated olefins, have been analyzed by Hammett plots (log k vs. σ_p^-) and lead to ρ values from 1 to 4.[11] Much larger ρ values have been reported for addition reactions following an anionic attack,[12] allowing one to unambiguously distinguish between the mechanisms. A log relative k_5 vs. σ_p^-[13] analysis of our largest data set (**3**) yields $\rho = 2.3$ with a reasonable correlation ($r = 0.90$) only if the α-substituted acceptors **3d** and **3f** are excluded. The appearance of the three classes in Figure 5 and the fact that α-substitution does not slow down the relative k_5 significantly are both related to steric effects occurring mainly at the attacked carbon of the activated double bond (in agreement with reports on nucleophilic Michael-type additions[12,14,15]). With the assumption of parallel slopes for the LFER, an average steric

(10) Substrates **3**, **4**, and **5** exhibit irreversible reduction due to fast chemical follow-up reactions. However, it is assumed in this argumentation that the reduction potential reflects the ease of introducing the first electron into the activated olefin.

(11) (a) Citterio, A.; Arnoldi, A.; Minisci, F. *J. Org. Chem.* **1979**, *44*, 2674. (b) Giese, B.; Meixner, J. *Chem. Ber.* **1981**, *114*, 2138.
(12) Charton, M. *Progress in Physical Organic Chemistry*; Streitwieser, A. S., Taft, R. W., Eds.; Wiley: New York, 1973; Vol. 10.
(13) Exner, O. *Correlation Analysis in Chemistry*; Chapman, N. B., Shorter, J., Eds.; Plenum: New York, 1978.
(14) Giese, B.; Lachhein, S. *Angew. Chem.* **1981**, *93*, 1016.
(15) Citterio, A.; Minisci, F.; Vismara, E. *J. Org. Chem.* **1982**, *47*, 81.

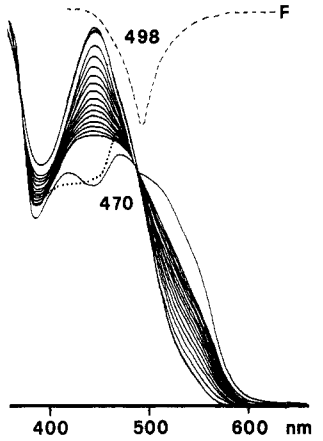

Figure 6. Changes in the visible spectrum of **2** (4.8×10^{-6} mol) in DMF upon irradiation with monochromatic light (498 nm, 3.3×10^{-9} einstein/s) in the presence of **3c** (0.44 M) followed by the slow transformation of the intermediate complex to vitamin B_{12r} (...): F, filter curve.

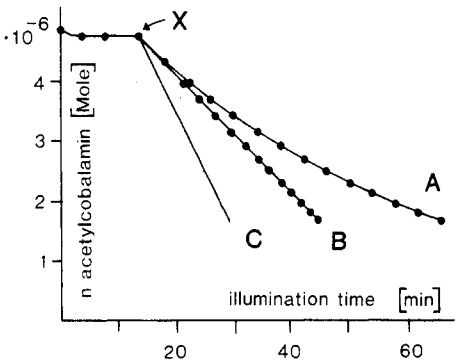

Figure 7. Plot of $n2$ (4.8×10^{-6} mol) vs. illumination time ($\sim 2 \times 10^{-6}$ einstein/10 min): uncorrected (A) and corrected for photons absorbed by product complex (B). Correction for filter effect, see Experimental Section. C: Theoretical slope for $\Phi = 1$. From the relation slope B/slope C Φ was calculated. X: addition of **3c** (0.44 M). Initial decay was due to traces of oxygen.

hinderance parameter E_s = log (rel k_5(**3**)/rel k_5(**4**)) = log (rel k_5(**4**)/rel k_5(**5**)) = 0.95 for the introduction of the first and second alkyl group can be calculated. The empirical law (eq 23) predicts the relative k_5 from $E_{1/2}$ and the number of substituents at the β-carbon (n_β).

$$\log \text{rel } k_5 = 1.33(E_{1/2} \text{ (vs. SCE)} + 2.00 \text{ V}) - 0.95n_\beta \quad (23)$$

Photolysis of Acetylcobalamin (2). Photolysis of **2** in the presence of different substrates was carried out to probe relative k_5 values (derived from current measurements) and to check the possibility of alternative mechanisms for step II/III. Crystalline **2**[16] dissolved in dimethylformamide exhibits a visible spectrum typical for acetylcobalamin in water with an uncoordinated dimethylbenzimidazole moiety (base off form, Figures 3 and 6).[17] If this carefully degassed solution is exposed to light, no decomposition of **2** is observed (well-preserved absorption at 444 nm, Figures 6 and 7). Upon addition of the activated olefin and continuous illumination at 498 nm, an isosbestic change in the visible spectrum for generally up to 80% of decomposition is observed. Plots of n acetylcobalamin vs. illumination time are exponential but become linear if corrected for the filter effect produced by the product complex.[18] From their slopes the quantum yield was calculated ($\Phi = n2$ photolyzed/n photons absorbed). Plots of Φ vs. [AO] are sigmoid and have been characterized for different activated olefins by their maximum quantum yield (Φ_{max}) and [AO] necessary for half Φ_{max}:$[AO]_{\Phi_{max/2}}$ (Figure 8 and Table I). Two plausible consecutive mechanisms (A and B) both give rise to a sigmoid dependence (eq 24 and 25). Mechanism A involves Co···Ac that may re-form the original Co–C bond or react with the activated olefin.[6] Φ_{max} is expected to be independent of Z. Mechanism B involves a photoexcited complex of intact acetylcobalamin and activated olefin as postulated for alkylcobalamins.[8d,19] Its unimolecular de-

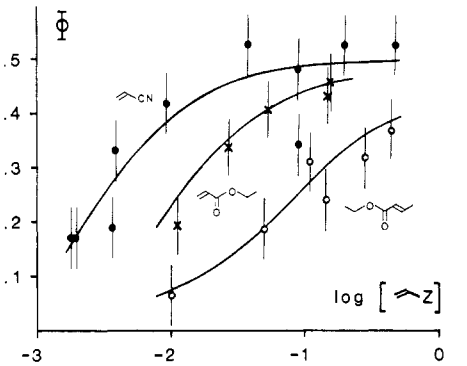

Figure 8. Correlation of Φ vs. log [AO]. Vertical bars indicate approximate errors due to light intensity fluctuation.

A. Quenching of Co···Ac

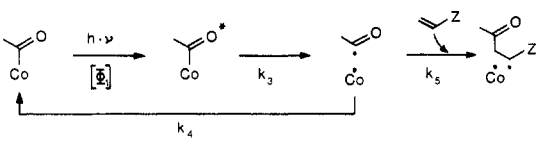

$$\Phi = dn\dot{C}o/Idt = \Phi_1 k_5[AO]/(k_5[AO] + k_4) \quad (24)$$
$$\Phi_{max} = \Phi_1$$
$$[AO]_{\Phi_{max/2}} = k_4/k_5$$

B. Fast Ground-State Complexation, Monomolecular Decomposition

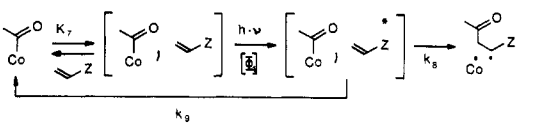

$$\Phi = dn\dot{C}o/Idt = \Phi_1 K_7[AO]/(K_7[AO] + 1)k_8/(k_8 + k_9) \quad (25)$$
$$\Phi_{max} = \Phi_1 k_8/(k_8 + k_9)$$
$$[AO]_{\Phi_{max/2}} = 1/K_7$$

(16) An electrochemical synthesis of **2** with a higher yield compared to that of the original procedure[6a] is described in the Experimental Section.

(17) **2** is known to exhibit in water a pH-dependent intramolecular base-on–base-off equilibrium of the benzimidazole residue connected with isosbestic changes in the electronic spectrum. We found its pK_a value (= 4.2 ± 0.05) in agreement with an approximate value from the literature[17a] and very close to the pK_a of free 1-α-D-ribofuranosyl-5,6-dimethylbenzimidazole (= 5.56),[17b] indicating little affinity of the central Co(III) atom in **2** toward complexation by the base. (a) Johnson, A. W.; Mervin, L.; Shaw, N.; Smith, E. L. *J. Chem. Soc.* **1963**, 4146. (b) Brown, K. L.; Hakimi, J. M.; Nuss, D. M.; Montejano, Y. D. *Inorg. Chem.* **1984**, *23*, 1463.

(18) No quenching processes are expected between photoexcited Co(II) and acetylcobalamin because their excited states are too short-lived.[7b] Al-Saigh, H. Y.; Kemp, T. J. *J. Chem. Soc., Perkin Trans. 2*, **1983**, 615.

(19) Fanchiang, Y.-T. *J. Chem. Soc., Chem. Commun.* **1982**, 1369.

(20) Doubly activated unsaturated products are reduced under conditions of catalysis.

(21) Insertion reactions of CO and O_2 into Co–C bonds of alkylcobalamins and model compounds have been noted. (a) Kräutler, B. *Helv. Chim. Acta* **1984**, *64*, 1053. (b) Jensen, F. R.; Kiskis, R. C. *J. Am. Chem. Soc.* **1975**, *97*, 5825.

(22) Reduction potentials of most alkylcobalamins: −1.5 V vs. SCE. Lexa, D.; Savéant, J. M. *J. Am. Chem. Soc.* **1978**, *100*, 3220. Pratt, J. M. *Inorganic Chemistry of Vitamin B_{12}*; Academic: London, New York, 1972. Coulometric results (n_e = 1.2) indicate that during catalysis in dimethylformamide with a natural dimethylamine content both homogeneous and electrochemical reduction are effective.

composition competing with deactivation leads to a Φ_{max} depending on k_8 and/or k_9, implying that the type of acceptor influences Φ_{max}. Our experimental Φ_{max} values differ but within experimental error and do not allow us, therefore, to distinguish between mechanisms A and B. We could not find any spectroscopic evidence for ground-state complexation (excimer formation is not compatible with the lifetime of photoexcited alkylcobalamins). On the basis of mechanism A and according to eq 24, $-\log [AO]_{\Phi_{max/2}} = \log k_5 - \log k_4$ should be proportional to log rel $k_5 - \log k_4$ (eq 18). The correlation of $-\log [AO]_{\Phi_{max/2}}$ vs. log rel k_5 exhibits a best fit straight line with a slope of 1.11 and $r = 0.975$, indicating inherent consistency in the two sets of data.

The final spectrum observed after complete photolysis of acetylcobalamin in freshly distilled dimethylformamide or dimethyl sulfoxide is definitely not due to vitamin B_{12r} (Figure 6). If at this point a hydrogen donor is added, the spectrum of B_{12r} (470 nm) develops isosbestically in the dark. If photolysis is started in the presence of both activated olefin and an hydrogen donor, direct conversion of **2** to B_{12r} with the same quantum yield is observed (no photolytic decomposition of **2** occurs if only the amine is present). According to eq 26 the formation of organic coupling products resulting from photolysis of **2** is clearly enhanced in the presence of a hydrogen donor. Cyclic

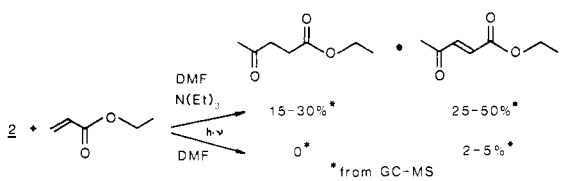

(26)

voltammetry of **2** photolyzed in dimethylformamide of low amine content shows an approximately 1.6-fold cathodic current on the first scan for the redox couple at –0.7 V and almost no current for the Co(II)/Co(III) oxidation (Figure 9). Once reduced at the electrode or after addition of triethylamine, a cyclic voltammogram typical for B_{12r} is obtained. The B_{12} intermediate observed after the noncatalytic photolysis of **2** has either an oxidized macrocycle or metal as compared to B_{12r}. Either site of oxidation may be due to an initially formed product radical. It may have abstracted a hydrogen atom from the macrocycle[23] or reformed a Co–C bond. In the first case, the increased cathodic current is due to the reduction of the macrocycle. In the latter case, a formal insertion of the olefin into the Co–C of acetylcobalamin generates a new alkylcobalamin.[21] Its chemical or electrochemical reduction at a surprisingly positive potential[22] liberates the preformed organic product by reductive cleavage of the Co–C bond. This hypothesis accounts for the increased amount of organic coupling products observed in the noncatalytic decomposition of **2** in the presence of triethylamine and Michael olefin (eq 26). The unsaturated products may be formed by a base-induced fragmentation of the alkylcobalamins competing with their reductive cleavage. Under the conditions of catalysis no unsaturated products are observed. If they are formed during catalysis, they would irreversibly be reduced at the electrode.

Concluding Remarks

The method developed in this work for the determination of kinetic data is based on a steady-state treatment

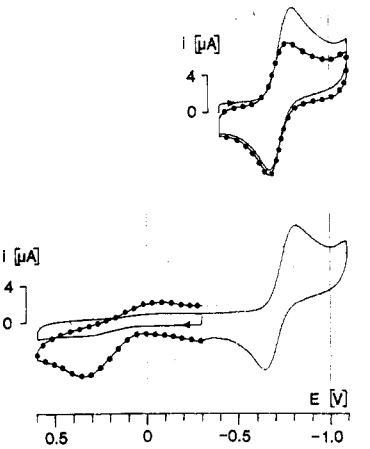

Figure 9. Cyclic voltammogram of **2** (0.7 mM) photolyzed in presence of **3c** in DMF/TBAP (0.1 M) obtained on a glassy carbon electrode at $v = 50$ mV s^{-1} (vs. SCE). Increased cathodic current on the Co(II)/Co(I) wave and only traces of the Co(II)/Co(III) couple are observed on the first scan. Dotted line: CV obtained on the second scan.

of the catalytic cycle (Scheme I). From the dependence of the catalytic current on substrate concentration or light intensity the proposed mechanism has been checked. Individual rate constants and the quantum yield became experimentally accessible even under combined limiting conditions. Kinetic data determined in this way describe for the first time quantitatively in terms of linear free energy relationships the reactivity of a photoexcited acylcobalamin toward activated olefins. The nucleophilic character of the Co-stabilized acyl moiety could be established ($\rho = 2.3$) and is in the same range as noted for alkyl radical additions to activated olefins. The steric hinderance exhibited by β-methyl substituents on the olefin is similar to reported values for radical or ionic Michael additions. However, in contrast to so-called "free" acyl radicals which decay in the absence of a suitable reaction partner, virtually no decomposition of photoexcited acetylcobalamin is observed if no olefinic quencher is present. This fact accounts for the high yields and substrate selectivity known for the B_{12}-catalyzed nucleophilic acylation under visible light illumination. The rate-limiting attack of the olefin on acetylcobalamin after photoexcitation is observed by both methods, catalysis and noncatalytic photolysis of acetylcobalamin. However, only the latter method indicates a complicated mechanism for reaction 5 in Scheme I, involving a formal insertion reaction of the olefin into the Co–C bond with product release only upon reduction of this organometallic intermediate or a hydrogen abstraction from the B_{12} ligand system. Current studies, which are subject of a forthcoming publication, have strengthened the insertion hypothesis.

Experimental Section

Materials. All physical measurements with dissolved **2** were performed with rigorous exclusion of oxygen. The argon was purified with BTS catalyst (BASF) in conjunction with molecular sieves. Dimethylformamide (Fluka, puriss.) used as a solvent for the photolysis of **2** was stored over molecular sieves and distilled freshly over P_2O_5 under reduced pressure. For the catalytic experiments it was used as purchased. The activated olefins (Fluka, puriss. or purum except **1d**, **2d**, **3b**, and **3d**, which were of practical quality) were distilled before use and purity-checked by ^{1}H NMR or GC. **3a** was prepared by oxidation of 2-methyl-3-buten-2-ol with PCC following a literature procedure[24]

(23) The involvement of hydrogen atoms originating from the corrin macrocycle during photolysis of alkylcobalamins has been proposed.[6c] Maillard, P.; Giannotti, C. *J. Organomet. Chem.* **1979**, *182*, 225.

(24) Dauben, W. G.; Michno, D. M. *J. Org. Chem.* **1977**, *42*, 682.

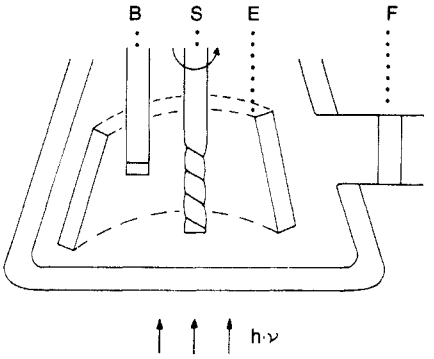

Figure 10. Illuminated cathodic compartment of the cell used for synthesis and mechanistic studies: E, graphitized carbon felt[25] (1.1 g, 4300 cm^2); S, stirrer; B, salt bridge; F, fritted glass.

(^{1}H NMR purity 96% (4% unreacted alcohol, which was not active as a quencher in a blank experiment)). **3c** was prepared by esterification of senecioic acid (GC purity 99%). The stereochemistry of the acyclic 3-monosubstituted olefins **2a,b,e** was trans. Lithium perchlorate (Fluka, puriss.) was used as electrolyte without further purification, whereas tetrabutylammonium perchlorate (Fluka, purum) was twice recrystallized from ethyl acetate.

Instruments and Apparatus. ^{1}H NMR spectra were recorded on a Varian EM 360 spectrometer. Infrared spectra were obtained on a Perkin-Elmer 782 IR spectrophotometer. FAB-mass spectra were recorded on a VG ZAB 2F instrument using Ar bombardment at 4 kV and GC–mass spectra on a MAT 44S with data system SS 200. The potentiostat and function generator used for electrolysis or cyclic voltammetry were Models 173/179 and 175 from Princeton Applied Research. Half-wave potentials of the activated olefins were measured at the dropping mercury electrode with a Metrohm Polarorecord E 506 in differential pulse mode. The electrochemical cell was a conventional glass frit (F), separated H-type, thermostated at 22 °C, and illuminated from the bottom as shown in Figure 10. The cathode (E) consisted of a hollow cylindrical piece of graphitized carbon felt[25] (1.1 g $\approx$ 4300 cm^2, GFA5 Sigri Elektrodengraphit GmbH, Meitingen, FRG). Constant convection of the 45–50-mL catholyte (dimethylformamide/$LiClO_4$, 0.2 M) by mechanical stirring (S) and a potential of −1.1 V vs. SCE via a salt bridge (B) was applied. This configuration yielded $DA/V_c\delta = 3.6 \times 10^{-3}$ s^{-1} from the slope of the linear ln i vs. t plot for the reduction of vitamin B_{12r} to B_{12s} (4.5×10^{-3} M) in the current range 40–2 mA. The light flux into the cells was determined by ferrioxalate actinometry[26] at 405 and 453 nm and was measured with a thermopile at other wavelengths.

Light Intensity, Wavelength, and Substrate Concentration Dependence of $i_{cat.}$. The computer-controlled optical and data acquisition system has been described recently by G. Calzaferri.[27] We used his original arrangement of the Xenon lamp, monochromator, light intensity and wavelength control, and computerized A/D conversion. The cell was protected from daylight by a black box with a shutter controlled aperture. The monochromatic light beam (30-nm band width, $d \approx 1$ cm) was guided onto the aperture and through the bottom of the cathode compartment (Figure 10) to reach the dissolved catalyst (4×10^{-3} M). Throughout an experiment to measure either wavelength or light intensity dependence of the catalytic current, substrate concentration of acetic anhydride (0.21 M) and acrylonitrile (0.30 M) remained essentially unchanged. The wavelength dependence of $i_{cat.}$ was studied at a constant light energy (1.54×10^{-8} einstein/s at 405 nm) with nine 30-nm steps from 640 to 370 nm, each step consisting of an illumination period of 25 min, assuring that the steady state was established, followed by a dark period of 45 min during which the current decreased to background values of <0.1 mA. The intensity dependence of $i_{cat.}$ was carried out at 490 nm with stepwise increased photon flux from 0.19 to 2.67×10^{-8} einstein/s. Illumination times of 20 min and dark periods of 45 min were used. The same photoelectrochemical cell as described above was used for the substrate dependence of $i_{cat.}$. The light source was a 300-W halogen lamp of unknown absolute intensity with a reflector 20 cm from the cell bottom. Upon stepwise addition of appropriate amounts of oxygen-free substrates (0.02–2 mL/step), the catalytic current and its integration were observed until i_{cat} was constant in each case (15 min). For small concentrations and large currents the substrate consumption was taken into account for $1/[(AC)_2O]$ or $1/[AO]$ vs. $1/i_{cat.}$ plots.

Synthesis of Acetylcobalamin (2). The electrosynthesis was carried out in a conventional H-type cell with a fritted glass separation at a stirred mercury pool (12 cm^2) under potentiostatic conditions. The cathodic and anodic compartments were filled with 20 and 10 mL of degassed solutions of $LiClO_4$ (0.3 M) in methanol–water (1:1, v/v). After addition of 1.383 g of hydroxocobalamin hydrochloride (1 mmol; **1**) a potential of −1.2 V (vs. SCE) was applied. The current decreased exponentially to 1.5 mA, and the color of the solution became dark brown-green. At this point 250 coulombs were consumed (78% current yield for a two-electron process). The whole cell then was placed in an ice bath and protected from light, and, holding the electrode potential at −1.2 V, 1 mL of freshly distilled oxygen-free acetic anhydride was added. After 2 h 150 mL of oxygen-free acetone was added. **2** was obtained as orange-red crystals after 15 h at 4 °C, washed with acetone, and dried in vacuo (yield 1.327 g (97%)). The 90% pure crude **2**—as judged by visible spectroscopy—was separated from unacetylated vitamin B_{12} by column chromatography (7 cm^3 of CM-cellulose, 150 mL of oxygen-free water for 200 mg of crude **2**): UV/vis (neutral H_2O, $c = 2.4 \times 10^{-4}$ M) 248 (ϵ 4.33), 276 (sh, 4.26), 286 (4.18), 320 (4.12), 350 (4.10), 422 (3.70), 456 (3.73), 510 nm (3.88); UV/vis (0.1 M CF_3COOH, $c = 2.4 \times 10^{-4}$ M) 300 (ϵ 4.27), 308 (4.27), 348 (4.01), 444 nm (4.02); UV/vis (DMF, $c = 0.91 \times 10^{-4}$ M): 292 (ϵ 4.24), 312 (4.24), 352 (sh 4.02), 450 nm (3.95); $pK_a = 4.2 \pm 0.05$ (from absorbance vs. pH plot at 510 and 444 nm, isosbestic points = 331, 384, and 481 nm); IR (KBr) 3360, 3200, 2970, 2940, 1725, 1668, 1620, 1570, 1492, 1478, 1450, 1403, 1352, 1220, 1152, 1120, 1108, 1070, 995, 902, 870, 848, 810, 620, 562 cm^{-1}; FAB-MS, m/e (relative intensity) 1375 (35, $M^+ + 3$), 1374 (73, $M^+ + 2$), 1373 (78, $M^+ + 1$), 1372 (32, M^+), 1332 (79, $M^+ + 3 - CH_3Co$), 1331 (100, $M^+ + 2 - CH_3CO$), 1330 (92, $M^+ + 1 - CH_3CO$), 1329 (32, $M^+ - CH_3CO$). Anal. Calcd for $C_{64}H_{91}N_{13}O_{15}PCo \cdot H_2O$: C, 55.29; H, 6.74; N, 13.10. Found: C, 55.32; H, 7.03; N, 12.78.

Rate of Acetylation of Vitamin B_{12s} by $(Ac)_2O$. Solutions of vitamin B_{12s} (0.002 M) in DMF/0.2 M TBAP were prepared by bulk electrolysis. Upon addition of $(Ac)_2O$ (0.028, 0.051, 0.202 M) [Co(I)] was determined from the anodic current of cyclic voltammograms on the Co(I)/Co(II) wave. Plots of log [Co(I)] vs. t were linear for approximately 1–1.5 half-lives with negative slopes proportional to $[(Ac)_2O]$. From the initial gradients an average $k_1 = 0.021$ M^{-1} s^{-1} was calculated.

Photolysis of 2. Photocell and cuvette ($d = 0.2$ cm) formed a closed air-tight removable system. Dry acetylcobalamin (**2**) (4–10 mg ($2.9–7.3) \times 10^{-6}$ mmol) was introduced. Dimethylformamide (8–10 mL) was degassed in the presence of ultrasound prior to filling the cell under an argon atmosphere. Liquid substrates were introduced in dark periods between illumination steps with a syringe through an argon-flushed stopcock on the cell with negligible oxygen contamination of the cell content as checked by blank experiments. The optical set up consisted of a 50-W halogen lamp, a condenser, and a 498-nm interference filter (Baizers, 30-nm half-width). The light beam ($d = 1$ cm) entered the coaxially mounted cylindrical photocell ($L = 4$ cm, $d = 1.7$ cm) with a calibrated light flux of $(1.2–3.5) \times 10^{-9}$ einstein/s, as determined by actinometry. Complete light absorption (>99.9%) by the magnetically stirred solution of **2** ($(4–8) \times 10^{-4}$ M) occurred within 0.7–1.5 cm. Alternatively, ca. 20 illumination steps (m = step number, 2–10 min each) and a visible spectra recording have been performed. n_t was calculated according to $n_t = c_i V(A_t - A_f)/(A_i - A_f)$ with n_t = moles of **2** present at illumination time t, A_i and A_f = initial and final absorbances, respectively, A_t = absorbance at time t, c_i = initial concentration of **2**, and V = volume of the solvent. Plots of n_t vs. t showed an exponential behavior due to

(25) Ruhe, A.; Walder, L.; Scheffold, R. *Helv. Chim. Acta* **1985**, *68*, 1301.
(26) Parker, C. A. *Photoluminescence of Solutions*; Elsevier: Amsterdam, London, N.W., 1968.
(27) Calzaferri, G.; Hug, S.; Hugentobler, T.; Sulzberger, B. *J. Photochem.* **1984**, *26*, 109.

the filter effect of the product complex. It was eliminated by stepwise correction of the illumination time assuming an isosbestic point at 498 nm according to

$$t' = \sum_{m=1}^{m(\max)} (t_m - t_{m-1}) n_{m'}/n_i$$

where t' = corrected (unfiltered) illumination time, m = illumination step number, $n_{m'}$ = moles of **2** present at the extrapolated halftime between t_m and t_{m-1}, and n_i = moles of **2** initially present. Plots of n_t vs. t' gave straight lines. From their slopes the quantum yield of the zero-order decomposition of **2** was calculated.

Acknowledgment. We thank the Swiss National Science Foundation for financial support. We thank Prof. R. Scheffold (Bern) for helpful discussions and Prof. G. Calzaferri (Bern) for making his photochemical instruments available to us.

Registry No. **2**, 18195-23-8; **3a**, 107-02-8; **3b**, 78-94-4; **3c**, 107-13-1; **3d**, 126-98-7; **3e**, 140-88-5; **3f**, 97-63-2; **3g**, 79-06-1; **4a**, 123-73-9; **4b**, 497-03-0; **4c**, 930-30-3; **4d**, 930-68-7; **4e**, 623-70-1; **5a**, 107-86-8; **5b**, 141-79-7; **5c**, 638-10-8; **5d**, 4786-24-7; B_{12s}, 18534-66-2; hyroxocobalamin hydrochloride, 58288-50-9; acetic anhydride, 108-24-7.

(η^2-Olefin)(1,4-diaza-1,3-diene)dicarbonyliron Complexes. 1. Preparation and Dynamic NMR Spectroscopic Properties

Hans-Werner Frühauf,* [1a] Ingrid Pein, and Frank Seils [1b]

FB 6—Fachgebiet Organische Chemie der Universität GH Duisburg, D-4100 Duisburg 1, Bundesrepublik Deutschland

Received October 30, 1986

The reaction of (η^4-diethyl muconate)(dad)Fe(CO) complexes (dad = 1,4-diaza-1,3-diene) with CO results in stepwise decoordination of the muconate ligand. The rates of the two consecutive displacement steps strongly depend on the properties of the respective dad ligands. Two examples of the intermediate (η^2-muconate)(dad)$Fe(CO)_2$ complexes were isolated. The complexity of their temperature-dependent NMR spectra precluded an analysis of the underlying dynamic processes. Photochemically, a series of analogous η^2-monoolefin complexes has been prepared. At low temperatures, in the rigid limiting case, their spectra are consistent with a trigonal-bipyramidal arrangement where the olefin is in equatorial position, while the dad nitrogen atoms and the two carbonyl groups occupy axial/equatorial positions, resulting in overall C_1 symmetry. A dynamic exchange process, observed in all cases, consists in rotation of the olefin about the bond to iron. With cis-disubstituted olefins, having local C_s symmetry when coordinated, simultaneous mutual exchange of the CO ligands, the dad halves, and the olefin halves is observed. This agrees with a Berry pseudorotation process, where olefin rotation occurs in the apical position of the intermediate square-pyramidal arrangement of overall C_s symmetry. The activation barriers depend (i) on the extent of π-back-bonding to the olefin, which, for a given olefin, is reduced when the more π-acidic dad ligands compete for the electron density at iron, and (ii) on the steric bulk of dad and olefin ligands. In cases where the olefin and the (dad)$Fe(CO)_2$ fragments have no symmetry element in common, a second exchange process at higher temperatures is observed which again equilibrates the two inequivalent halves of the dad ligand. This exchange cannot be effected by the former mechanism. Of the possible explanations being discussed for this second dynamic exchange process, a reversible dissociation of the olefin is strongly favored.

Introduction

Our continuing interest in the preparation, structural elucidation, investigation of spectroscopic properties, and reactivity patterns of (1,4-diaza-1,3-diene)carbonyliron complexes with organic π-ligands originates in their close relation to known active species in dad–Fe systems[2] that homogeneously catalyze the dimerization or oligomerization of unsaturated organic molecules. In the square-pyramidal coordination geometry of (η^4-1,3-diene)(dad)-carbonyliron complexes **1**,[3] we have observed an interesting dependence of ligand arrangement on the π-acidity of the diene ligand. With diethyl muconate, a pronounced π-accepting diene, the two nitrogen atoms of all types of dad ligands (cf. Chart I) are coordinated in basal/apical positions, reducing the symmetry of the complex to C_1. Complexes with dienes without electron-withdrawing substituents exhibit C_s symmetry, due to N,N′ basal/basal coordination of the respective dad ligands. The latter complexes **1**-C_s are unreactive with respect to ligand substitution reactions, while the complexes **1**-C_1, with diethyl muconate, show strongly increasing substitutional lability with increasing acceptor properties of the dad ligands, e.g.,

Chart I

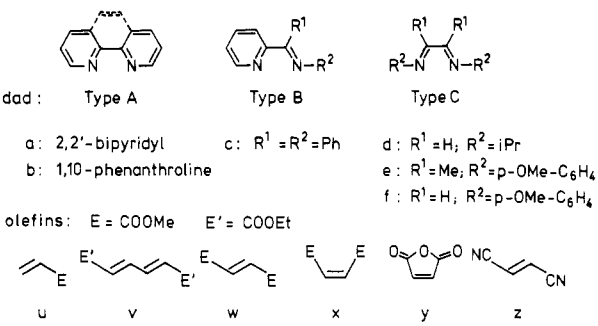

(1) (a) New address: Laboratorium voor Anorganische Chemie, University of Amsterdam, J.H. van't Hoff Instituut, Nieuwe Achtergracht 166, 1018 WV Amsterdam, The Netherlands. (b) Present address: Department of Chemistry, The University of Alberta, Edmonton, Alberta, Canada T6G 2G2.

(2) (a) Yamamoto, A.; Morifuji, K.; Ikeda, S.; Saito, T.; Uchida, Y.; Misono, A. *J. Am. Chem. Soc.* **1965**, *87*, 4652. (b) *Ibid.* **1968**, *90*, 1878. (c) Misono, A.; Uchida, Y.; Hidai, M. *Bull. Soc. Chem. Jpn.* **1966**, *39*, 2425. (d) Wu, Ch.-Y.; Swift, H. E. *J. Catal.* **1972**, *24*, 510. (e) Maly, N. A.; Menapace, H. R.; Benner, G. S.; Hillegas, D. V. *ACS Symposium on New Routes to Olefins*; Boston, April 1973; Abstr. No. B95. (f) tom Dieck, H.; Bruder, H. *J. Chem. Soc., Chem. Commun.* **1977**, 24.

(3) Frühauf, H.-W.; Wolmershäuser, G. *Chem. Ber.* **1982**, *115*, 1070.

0276-7333/87/2306-1613$01.50/0